Bifunctional effects of carbon coating on high-capacity Li1.2Ni0.13Co0.13Mn0.54O2 cathode for lithium-ion batteries

ARTICLE *in* JOURNAL OF SOLID STATE ELECTROCHEMISTRY · APRIL 2015

Impact Factor: 2.45 · DOI: 10.1007/s10008-014-2707-5

6 AUTHORS, INCLUDING:

H.F. Xiang

Hefei University of Technology

38 PUBLICATIONS **1,025** CITATIONS

SEE PROFILE

J Solid State Electrochem (2015) 19:1027–1035
DOI 10.1007/s10008-014-2707-5

ORIGINAL PAPER

Bifunctional effects of carbon coating on high-capacity $Li_{1.2}Ni_{0.13}Co_{0.13}Mn_{0.54}O_2$ cathode for lithium-ion batteries

J. J. Chen · Z. D. Li · H. F. Xiang · W. W. Wu · X. Guo · Y. C. Wu

Received: 11 October 2014 / Revised: 3 December 2014 / Accepted: 9 December 2014 / Published online: 23 December 2014

Abstract Coating the Li-rich layered oxide cathode $Li_{1.2}Ni_{0.13}Co_{0.13}Mn_{0.54}O_2$ with small amount of conductive carbon is realized by low-temperature sucrose carbonization in air. Carbon coating gives rise to a small amount of Mn^{3+} on the surface of the $Li_{1.2}Ni_{0.13}Co_{0.13}Mn_{0.54}O_2$. The 1.2 wt% carbon-coated $Li_{1.2}Ni_{0.13}Co_{0.13}Mn_{0.54}O_2$ shows obviously enhanced electrochemical performances, especially in improving rate capability and suppressing the voltage fading during long-term and high-rate cycling. According to the analysis from cyclic voltammetry (CV) and electrochemical impedance spectra (EIS), the improvements on the electrochemical performances are mainly because the coated carbon layer can function by not only increasing the electronic conductivity at the interface with electrolyte but also improving bulk electronic and ionic conductivity by small amounts of Mn^{3+}. Therefore, carbon coating is a promising approach to improve the cyclic stability of the Li-rich layered oxides.

Keywords Lithium-rich layered oxide · Carbon coating · Lithium-ion batteries

J. J. Chen · Z. D. Li · H. F. Xiang (✉) · W. W. Wu · X. Guo · Y. C. Wu (✉)
Anhui Provincial Key Laboratory of Advanced Functional Materials and Devices, School of Materials Science and Engineering, Hefei University of Technology, Anhui Hefei 230009, People's Republic of China
e-mail: hfxiang@hfut.edu.cn
e-mail: ycwu@hfut.edu.cn

J. J. Chen
Department of Chemistry & Chemical Engineering, Anqing Normal University, Anhui Anqing 246011, People's Republic of China

Introduction

Further development of electric vehicles (EVs) and smart grids have stimulated the demand for advanced rechargeable batteries, among which lithium-ion battery (LIB) is the most promising candidates owing to its high energy density and successful commercialization in the portable electronic devices [1–3]. However, the presently available cathodes have a limited capacity (<200 mAh g^{-1}) [4–6]. Solid solutions between Li_2MnO_3 and $LiMO_2$ (denoted as $xLi_2MnO_3 \cdot (1-x)LiMO_2$, M=Ni, Co, Mn, or combinations), with a reversible capacity of ~250 mAh g^{-1}, is quite attractive to high-energy LIBs for EVs and smart grid applications [7–9]. However, their drawbacks of large irreversible capacity loss during the initial cycle and poor rate capability limit their commercial utilization. The large irreversible capacity in the initial cycle is attributed to the extraction of Li_2O followed by elimination of oxygen ion vacancies from the lattice for activation of Li_2MnO_3 component and formation of the thick cathode-electrolyte interface (CEI) layer [10–12]. The poor rate capability is possible resulting from the high-impedance CEI layer and the low electronic conductivity at the electrode/electrolyte interface [13–15]. It is obvious that the interfacial property significantly affects the electrochemical performance of the Li-rich layered oxides.

In our previous paper [12], CEI layer was optimized by introduction of trimethyl phosphite (TMP) as high-voltage electrolyte additive and the electrochemical performance and thermal stability of Li-rich layered oxide cathode were obviously improved. Besides the reformulation of the electrolytes, surface coating on the cathode material is an effective alternative to modify the CEI film between the Li-rich layered oxide and the electrolyte [16–18]. Surface coating by Al_2O_3 [16], CeO_2 [17] and AlF_3 [18] was proved to effectively reduce irreversible capacity loss in the first cycle and improve the cycle stability, but

depressed the electronic conductivity at the interface. Carbon is an ideal conductive coating agent because on one hand it can serve as protective layer to cover the active sites and reduce the contact between the active material and the electrolyte and on the other hand it can enhance surface electronic conductivity [19–22]. Carbon coating is widely used to enhance the electrochemical properties of phosphate-based cathode [23]. But for the metal oxide cathode containing high valance metal ions such as Mn^{4+}, when the carbon coating was conducted in a high-temperature condition, the high valance metal ions is easily to be reduced. At the same time, carbon coating has been found efficient to enhance cycling and rate performance of metal oxide cathode such as $LiMn_2O_4$ [24, 25], $LiNi_{0.5}Mn_{1.5}O_4$ [26], and $LiNi_{1/3}Co_{1/3}Mn_{1/3}O_2$ [27]. Recently, Manthiram et al. [19] reported that surface modification of the $Li[Li_{0.2}Mn_{0.54}Ni_{0.13}Co_{0.13}]O_2$ with carbon film enhanced the surface electronic conductivity by 40 % and thus improved the rate capability and cycling performance of the Li-rich cathode material. Tu et al. [20] claimed that the discharge capacity and cycling performance of carbon-coated $Li_{1.048}Mn_{0.381}Ni_{0.286}Co_{0.286}O_2$ were improved because carbon coating can protect the Li-rich cathode material from reacting with the electrolyte and retard the incrassation of the CEI film on the surface of oxide particles. In order to avoid carbon reducing Mn^{4+} at high temperature, both Manthiram and Tu coated the carbon film on Li-rich cathode material via a physical route. The former used thermal evaporation in a JEOL thermal evaporator with a vacuum of $\sim 10^{-7}$ Torr and the latter chose direct-current magnetron sputtering. However, Deng et al. [21] fabricated carbon-coated $Li[Li_{0.2}Mn_{0.54}Ni_{0.13}Co_{0.13}]O_2$ cathode by polymer pyrolysis in air, and that carbon-coated cathode exhibited the enhanced specific capacity and rate performance because of suppressing the formation of the thick solid electrolyte interfacial layer and partly reducing Li_2CO_3 impurity on the $Li[Li_{0.2}Mn_{0.54}Ni_{0.13}Co_{0.13}]O_2$ particle surface.

Basically, either physical or chemical carbon coating is effective to improve the performance of the Li-rich cathode materials, and especially the organics pyrolysis is the more facile and economic route for commercial production. However, the surface chemistry of the Li-rich cathode materials should be carefully investigated after the chemically carbon coating. Herein, we performed the carbon coating on the $0.5Li_2MnO_3{\cdot}0.5LiNi_{1/3}Co_{1/3}Mn_{1/3}O_2$ cathode (denoted as $Li_{1.2}Ni_{0.13}Co_{0.13}Mn_{0.54}O_2$, and abbreviated as LNCMO hereafter) by sucrose pyrolysis in air. It was found that chemical carbon coating has the bifunctional effects on the LNCMO cathode. On the one hand, it can increase the electronic conductivity at the interface with electrolyte because of the conductive nature of carbon. On the other hand, the introduction of Mn^{3+} from the carbon thermal reduction of small amount of Mn^{4+} can improve bulk electronic conductivity and ionic conductivity of LNCMO. So, the optimal carbon-coated LNCMO (abbreviated as C-LNCMO hereafter) exhibits not only obviously reduced initial irreversible capacity loss and improved rate capability but also suppressed the voltage fading during long-term and high-rate cycling.

Experimental

Materials preparation

The pristine LNCMO was synthesized by a coprecipitation method combined with a solid-state reaction. The coprecipitation of the carbonate precursor was carried out as follows: 2 M Na_2CO_3 solution and 0.2 M ammonium hydroxide were simultaneously added dropwise into a solution containing manganese, nickel, and cobalt sulfates with a total concentration of 2 M and stirred for 12 h under 60 °C. The carbonate precursor was washed with deionized water and vacuum dried at 100 °C for 24 h. The carbonate precursor was then mixed with lithium carbonate and decomposed at 500 °C for 5 h in air. The decomposed powder was then calcined at 900 °C for 12 h in air to obtain the pristine LNCMO. Surface coating of the LNCMO with carbon were carried out as follows: the pristine LNCMO was mixed with 1, 3, and 5 wt% sucrose, then heat up to 200 °C at a rate of 1 °C min^{-1} and then to 350 °C at a rate of 3 °C min^{-1} in air.

Characterization and electrochemical measurements

The crystalline structures of the pristine LNCMO and C-LNCMO were identified by X-ray diffraction (XRD) using a diffractometer (D/MAX2500 V, Cu Ka radiation). The diffraction patterns were recorded in the 2 theta range from 10° to 80°. The amount of carbon coated on the LNCMO was examined by a themogravimetric analyzer (TGA, Q5000). The particle size and morphology of the pristine LNCMO and C-LNCMO were observed by scanning electron microscopy (SEM, Hitachi, SU8020) and transmission electron microscopy (TEM, Hitachi, H800). X-ray photoelectron spectroscopy (XPS, ESCALAB250 with monochromatic Al Ka radiation) was performed to characterize the surface state of the obtained products.

The electrochemical properties of the cathode materials were evaluated in CR-2032 type cells assembled in the glove box (MBraun). In order to make the electrode laminate, a slurry containing 84 wt% active material, 8 wt% acetylene black, and 8 wt% polyvinylidene fluoride (PVDF) dispersed in N-methyl-2-pyrrolidinone (NMP) was cast onto an aluminum current collector. After vacuum drying at 70 °C, the laminate was punched into discs (Φ 14 mm) for assembling the coin cells. The mass loading in the electrode was

controlled at about 1.5 mg cm^{-2}. Celgard 2400 microporous polypropylene membrane was used as separator. Highly pure lithium foil was used as the counter electrode and reference electrode for the cell assembly. The electrolyte was 1 M $LiPF_6$/ethylene carbonate (EC) + dimethyl carbonate (DMC) (1:1 *w*/*w*). The cell performance of pristine LNCMO and C-LNCMO were evaluated on a multichannel battery cycler (Neware BTS2300). For activation, all the cells were initially cycled twice between 2.0 and 4.8 V at a current rate of 0.1 C (1 C=250 mA g^{-1}). Then the cycling tests were performed at a current rate of 0.5 C in the constant current–constant voltage (CC-CV) charge mode and constant current (CC) discharge mode between 2.0 and 4.6 V. Cyclic voltammograms (CV) were performed over the potential range of 2.0–4.8 V at a scanning rate of 0.2 to 0.8 mV s^{-1} on a CHI 604D electrochemical workstation (Shanghai Chenhua Instruments Co. Ltd.). The electrochemical impedance spectra of the cells were also measured on the CHI 604D electrochemical workstation with the frequency range of 1 MHz to 0.01 Hz and potential perturbation of 10 mV at the SOC (state of charge) of 50 %.

Results and discussion

Since the sucrose is selected as carbon source to modify the surface of the LNCMO, the amount of residual carbon with different sucrose dosage should be initially investigated. Figure 1 shows TG curves of the pristine LNCMO and the carbon-coated LNCMO prepared from 3 wt% sucrose coated LNCMO from room temperature to 750 °C in air. A small weight loss (<0.2 %) occurs at 80–180 °C for the pristine LNCMO due to the trace moisture in the material. However, the carbon-coated sample has two weight loss steps at 90–180 and 300–450 °C, respectively, with the total mass loss of 1.4 %. Both the samples have the comparative moisture, so the 1.2 wt% (1.4–0.2) more weight loss attributed to carbon oxidization in air [26]. It means 1.2 wt% carbon is coated on LNCMO from 3 wt% sucrose (this sample was denoted as 1.2 % C-LNCMO hereafter). Analogously, 1 and 5 wt% sucrose coating results in 0.4 and 2.0 wt% carbon residual (samples were denoted as 0.4 % C-LNCMO and 2.0 % C-LNCMO hereafter), respectively.

The X-ray diffraction patterns of the pristine LNCMO and 1.2 % C-LNCMO are shown in Fig. 2. All the major diffraction peaks can be indexed as a layered oxide lattice based on a hexagonal α-$NaFeO_2$-type structure with a space group R-3m [28]. Both (006)/(102) and (108)/(110) doublets are clearly split, suggesting that the material crystallized in the layered structure without formation of any spinel structure [29]. The weak peaks between 20 and 25° (marked by asterisk) are reflected by a monoclinic unit cell with a C2/m symmetry, due to a $LiMn_6$ cation arrangement that occurs in the transition metal layers of Li_2MnO_3 region. No peak of carbon is observed due to its low quantity and/or its amorphous nature, illustrating that the coating processes do not destroy the structure of the Li-rich layered oxides and no impurity appears in the XRD patterns.

The morphologies of the pristine LNCMO and 1.2 % C-LNCMO were investigated by SEM, as shown in Fig. 3. From Fig. 3a, b, the pristine LNCMO are block-like particles of 200–500 nm in size. As shown in Fig. 3c, d, some stuff can be found on the surface of the 1.2 % C-LMNCO. Moreover, the color change in our experiment from red-brown of pristine LNCMO to black of 1.2 % C-LNCMO also indicates that sucrose was carbonized and carbon is coated on the LNCMO particles. Figure 4 shows the TEM images of the pristine LNCMO and 1.2 % C-LNCMO particles. Compared with the smooth surface of the pristine LNCMO (Fig. 4a), amorphous carbon layer is coated on the surface of the 1.2 % C-LNCMO with a thickness of 10–30 nm (Fig. 4b). From the

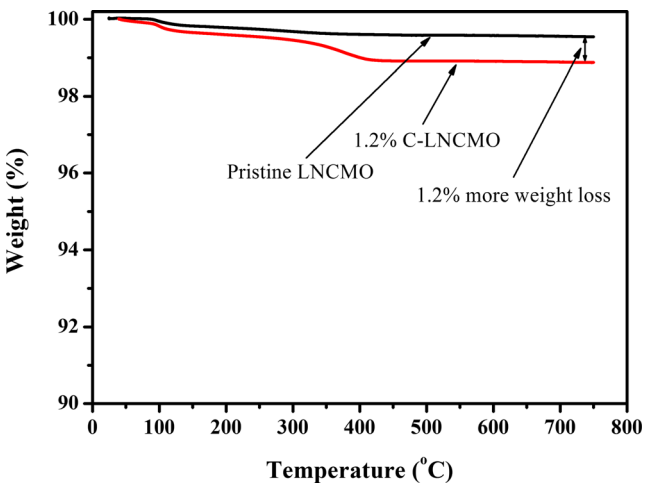

Fig. 1 TG curves of the pristine LNCMO and 1.2 % C-LNCMO

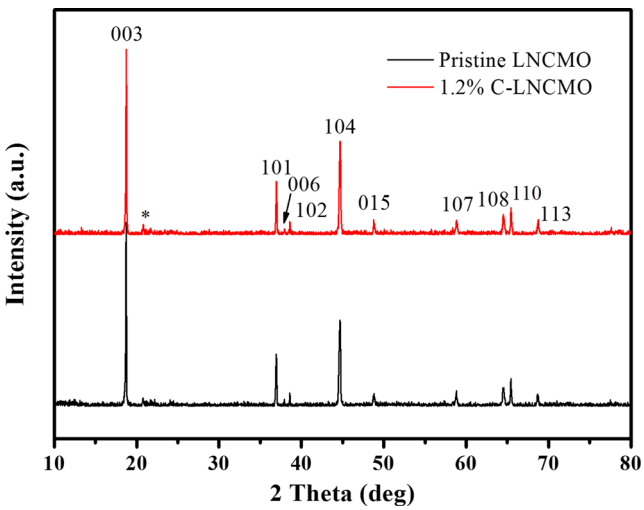

Fig. 2 XRD patterns of the pristine LNCMO and 1.2 % C-LNCMO

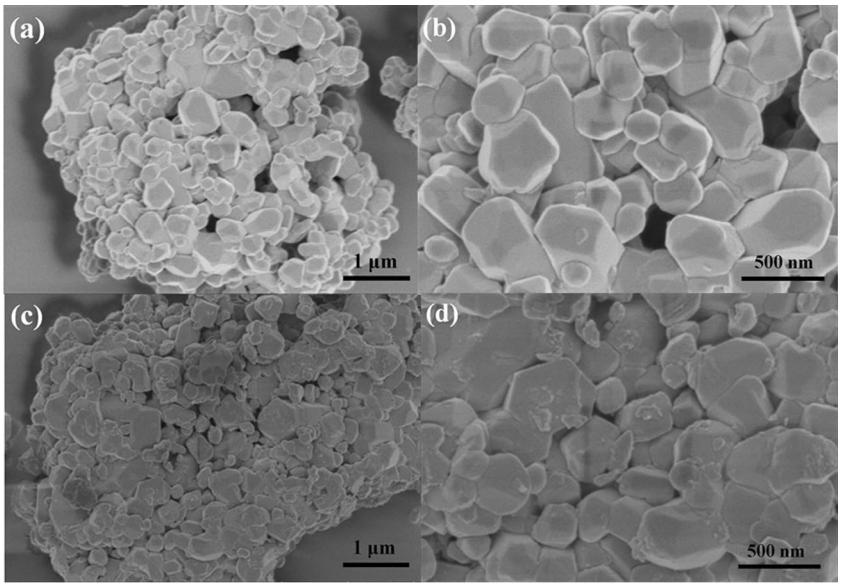

Fig. 3 SEM images of the pristine LNCMO (**a**) and 1.2 % C-LNCMO (**c**) at low magnification (×2.0k), the pristine LNCMO (**b**) and 1.2 % C-LNCMO (**d**) at high magnification (×5.0k)

SEM and TEM results, we expected that carbon layer could effectively decrease the direct contact area between the high-voltage cathode material and electrolyte.

It has been proved that the Mn^{4+} in LNCMO has the possibility to be reduced to Mn^{3+} by carbon in the process of sucrose carbonization, especially at the particle surface [26]. The oxidation state of Mn before and after carbon coating was investigated and the XPS spectra of the pristine LNCMO and 1.2 % C-LNCMO are shown in Fig. 5. These XPS spectra have been calibrated according to the binding energy of the C1s peak at 284.8 eV. As can be seen from Fig. 5a, the major binding energy peak of 642.7 eV corresponds to Mn^{4+} (assigned to Mn 2p3/2) in pristine LNCMO. According to the results showed in Fig. 5b, for the 1.2 % C-LNCMO, the existence of Mn^{3+} at energy peak of 642.0 eV (assigned to Mn 2p3/2) could be observed by peak separation and the amount of Mn^{3+} is 3.17 % determined from its corresponding peak areas [30]. This result confirms that carbon coating process gave rise to a small amount of Mn^{3+} on the surface of the 1.2 % C-LNCMO, which will contribute to higher bulk electronic conductivity and ionic conductivity owning to stronger conductivity and larger ionic radius of

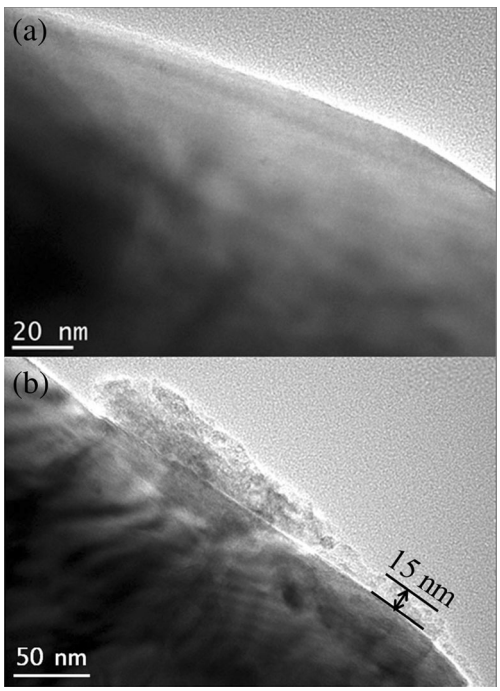

Fig. 4 TEM images of the pristine LNCMO (**a**) and 1.2 % C-LNCMO (**b**)

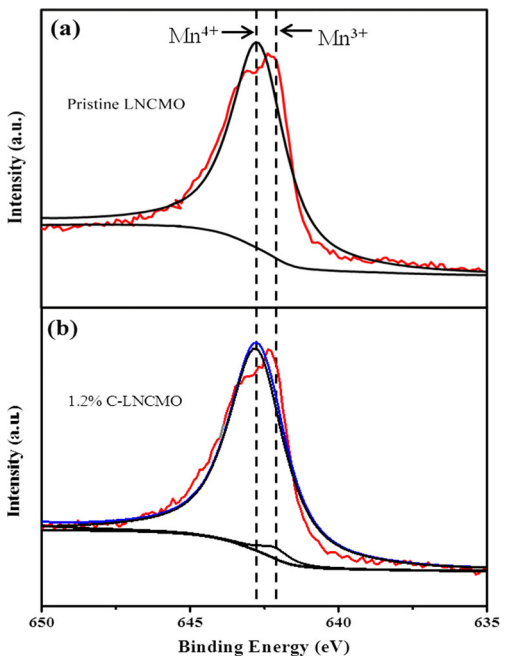

Fig. 5 XPS spectra of the pristine LNCMO (**a**) and 1.2 % C-LNCMO (**b**)

Mn^{3+} than those of Mn^{4+} [31]. During the reduction of Mn^{4+} into Mn^{3+}, the main reaction is possibly as $Mn(IV)O_x + y/2\ C = Mn(III)O_{x-y} + y/2\ CO_2$.

The initial charge and discharge curves and the cycling performances of the LNCMO with various amounts of carbon coating are shown in Fig. 6. As shown in Fig. 6a, all the samples show similar charge/discharge profiles. Table 1 compares the initial charge and discharge capacities and the irreversible capacity loss. The initial discharge capacity of the pristine LNCMO is 263.7 mAh g^{-1} with the irreversible capacity of 101.6 mAh g^{-1} and coulombic efficiency of 74.0 %. The 1.2 % C-LNCMO shows the highest discharge capacity (277.3 mAh g^{-1}) with the lowest irreversible capacity of 71.3 mAh g^{-1} and the highest coulombic efficiency of 79.5 %. It seems that coated carbon layer can suppress the loss of oxygen in the initial charge process so as to retain more oxygen vacancies in the bulk lattice to provide sufficient active sites for lithium ion insertion in the subsequent discharge process. Figure 6b shows the cycling performance of LNCMO with various carbon coating. After two formation cycles at 0.1 C, the discharge capacities of the different cells are quite close to 230 mAh g^{-1} at the third cycle. However, at the 80th cycle, the residual discharge capacities are 186.4, 189.9, 195.8, and 172.2 mAh g^{-1} for the pristine LNCMO, 0.4 % C-LNCMO, 1.2 % C-LNCMO, and 2.0 % C-LNCMO, respectively. It is obvious that appropriate amount of carbon coating improves the electrochemical performance of the LNCMO cathode materials by suppressing the side reactions between the active cathode materials and the electrolyte. The relatively low capacity of the 2.0 % C-LNCMO could be the result of structural instability induced by more Mn^{3+} introduced into the LNCMO lattice [17]. The discharge curves of the pristine LNCMO and 1.2 % C-LNCMO in the 3rd, 30th, and 75th cycles at 0.5 C are compared in Fig. 6c. It can be observed that voltage fading of the 1.2 % C-LNCMO is less serious compared with those of the pristine LNCMO during long-term cycling.

Figure 7 shows rate capability of the LNCMO with various amounts of carbon coating. After two formation cycles at 0.1 C, all the cells were charged at a rate of 0.5 C and discharged at incremental rates from 0.5 to 5 C then recovering back to 0.5 C. In the case of the pristine LNCMO, its discharge capacity decrease to 199.5, 176.4, and 137.1 mAh g^{-1} at 1, 2, and 5 C, respectively. However, the discharge capacities of the 1.2 % C-LNCMO are 203.9, 180.3, and 154.7 mAh g^{-1} at 1, 2, and 5 C, respectively. That is, appropriate carbon coating could improve the rate capability of the LNCMO. In addition, the discharge curves of the pristine LNCMO and 1.2 % C-LNCMO at 0.5, 2, and 5 C are compared in Fig. 7b. It is observed that for the pristine LNCMO besides the obvious capacity reducing, the discharge voltage fading is more and more serious with discharge rate increasing due to the Li^+ diffusion impedance in the bulk

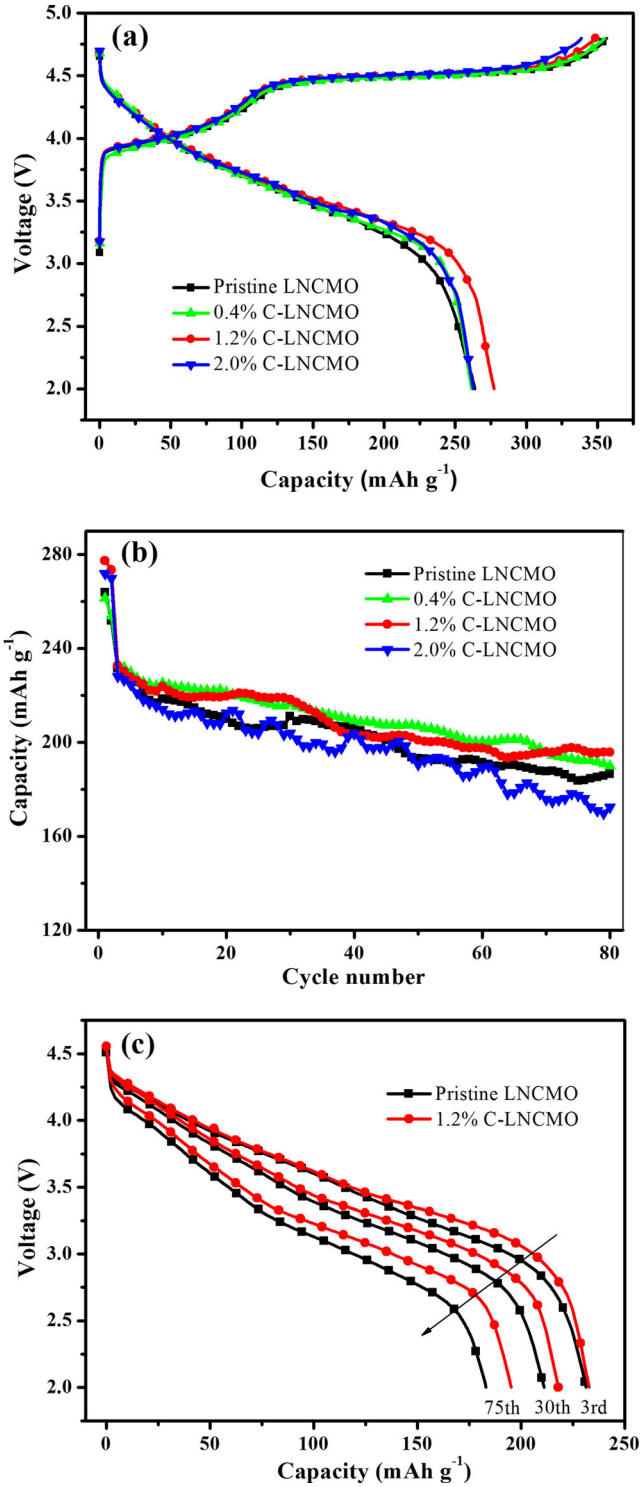

Fig. 6 Initial voltage profiles at 0.1 C (**a**), cycling performance at 0.5 C (**b**) of LNCMO with various amounts of carbon coating, and discharge curves of the pristine LNCMO and 1.2 % C-LNCMO electrodes (**c**)

LNCMO [32]. 1.2 % carbon coating can suppress not only the capacity reducing but also the voltage fading. According to the previous literature [33, 34], the voltage fading has been attributed to the formation of a spinel-like phase. Surface coating oxides/phosphates and electrolyte additives have been

Table 1 Information of the initial charge and discharge performances of LNCMO with various amounts of carbon coating

Samples	First charge capacity (mAh g^{-1})	First discharge capacity (mAh g^{-1})	Irreversible capacity loss (mAh g^{-1})
Pristine LNCMO	356.3	263.7	101.6
0.4 % C-LNCMO	355.0	261.4	93.6
1.2 % C-LNCMO	348.6	277.3	71.3
2.0 % C-LNCMO	338.7	262.7	76.0

used to stabilize the capacity of cathode materials and enhance cycling ability, but have little-to-no effect on voltage fading [34]. Herein, introduction of Mn^{3+} is apt to stabilize the structure during cycling, which could mitigate the layered oxide transformation into the spinel phase.

CV is a useful tool to study the oxidation/reduction and/or phase transformation processes in electrode reactions and to estimate the chemical diffusion coefficient of lithium ion. Figure 8 shows the initial CV curves of the pristine LNCMO and 1.2 % C-LNCMO measured at the sweep rates of 0.1, 0.2, 0.5, and 0.8 mV s^{-1}, respectively. The anodic peaks of both samples around 4.1 V are due to the oxidation process of Ni^{2+} and Co^{3+} to higher oxidation states, while the second anodic peaks above 4.5 V are normally associated with the Li_2O removal from the layered lattice. During cathodic reactions, the broad peaks between 4.3 and 3.2 V are regarded as the reduction processes of Ni^{4+} and Co^{4+}, while another peak

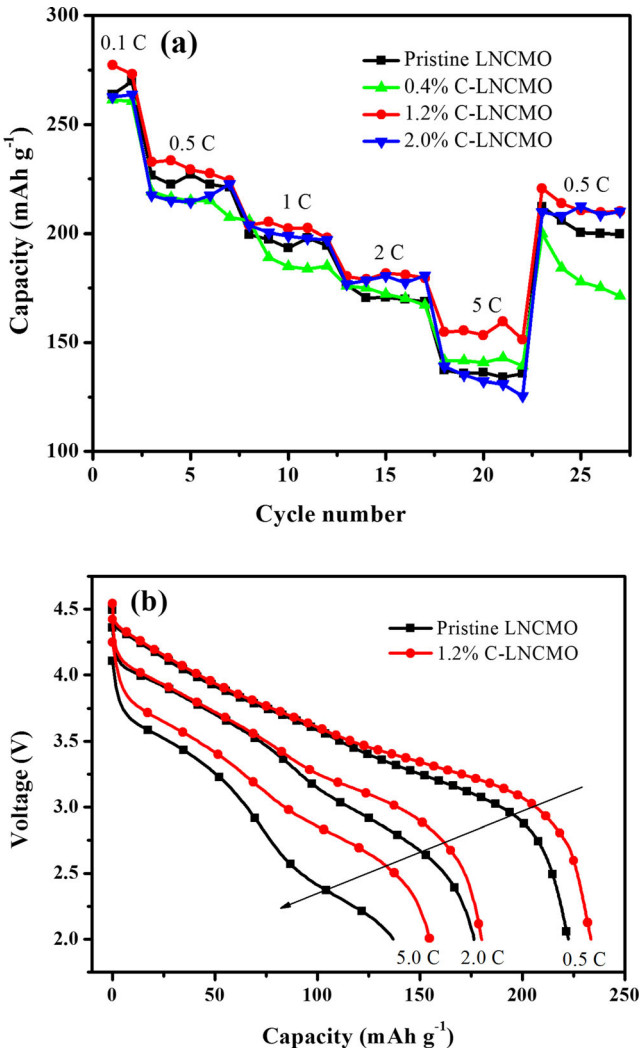

Fig. 7 Rate capability of LNCMO with various amounts of carbon coating (**a**), and discharge curves at various C rates of the pristine LNCMO and 1.2 % C-LNCMO electrodes (**b**)

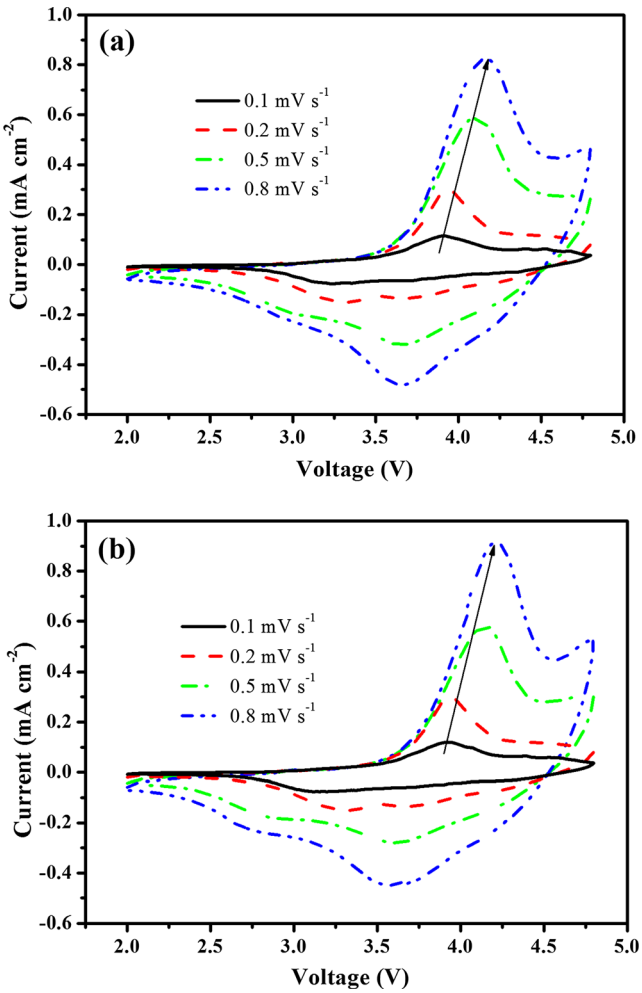

Fig. 8 Cyclic voltammetry of the pristine LNCMO and 1.2 % C-LNCMO electrodes at a series of sweep rates

around 2.7 V is believed to be due to insertion of Li^+ accompanied with Mn^{4+} reduction in surface spinel component [14, 30]. As the sweep rate increases, the anodic peaks shifted to higher potential and the corresponding cathodic peaks to lower potential, indicating that the irreversible behaviors become more manifest at higher sweep rates, in agreement with the voltage fading. The irreversibility is caused by the polarization that originates from either the incomplete extraction/insertion from/into the electrode of Li^+ during the time interval of a higher rate sweep or the slow electronic transfer [30]. It is interesting to point out that more apparent cathodic peaks around 2.7 V of 1.2 % C-LNCMO is associated with the Mn^{4+}/Mn^{3+} redox reaction, which is beneficial to mitigate voltage fading during cycling [35, 36]. Thackeray proposed the possible existence of a "layered-spinel-rocksalt" composite structure to minimize transition metal ion diffusion between the close packed layers of the oxygen sublattice during cycling [36].

Figure 9 presents the relationship between the anodic peak current and the sweep rate. As can be seen, the peak current shows a square root dependence on the sweep rate. This behavior is expected for a diffusion-controlled process in electrode [26], therefore the relationship of the peak current (I_p) and the sweep rate can be expressed as Eq. 1 [37]:

$$I_p = 2.69 \times 10^5 n^{3/2} A D_{Li^+}{}^{1/2} C_{Li} \nu^{1/2} \quad (1)$$

where I_p is the peak current (A, directly obtained from CV curves), n is the charge-transfer number, A is the surface area of the electrode (1.54 cm^2), C_{Li} is the concentration of lithium ions in the electrode (2.98×10^{-3} mol cm^{-3}, calculated from the volume of LNCMO (401.6 $Å^3$)), and ν is the potential scan rate (V s^{-1}). $D_{Li}{}^+$ is the diffusion coefficient and that of the pristine LNCMO and 1.2 % C-LNCMO could be calculated to be 5.6×10^{-10} and 6.8×10^{-10} cm^2 s^{-1}, respectively. It is apparent that the kinetics of Li^+ diffusion can be improved by 1.2 % carbon coating. It is reasonable that small amount of Mn^{3+} in the 1.2 % C-LNCMO contributes to higher bulk electronic conductivity and ionic conductivity and eventually improves the rate capacity.

EIS test was carried out to further understand the effect of carbon coating on the LNCMO electrodes. Before the EIS measurement, the cells were subjected to three galvanostatic charge–discharge cycles for activating and stabilizing the electrodes. Figure 10 shows the Nyquist plots of the pristine LNCMO and 1.2 % C-LMNCO electrodes at the SOC of 50 %. As shown in Fig. 10, Nyquist plots for both samples have two semicircles in the mid- and high-frequency regions and a straight line in the low-frequency. EIS results were fitted by using an equivalent circuit, in which R_e, R_f, R_{ct}, and W stand for internal resistance of the cell, the impedance of Li^+ diffusion in the interface (herein CEI) film, the impedance of charge transfer and Warburg impedance, respectively [38, 39]. The fitted impedance parameters of the equivalent circuit are listed in Table 2. The value of R_e of the 1.2 % C-LNCMO is relatively smaller than that of the pristine LNCMO, which suggests that the 1.2 wt% carbon coating can suppresses the growth of CEI film on the LNCMO surface. The value of R_f of the 1.2 % C-LNCMO (34.650 Ω) much lower than that of the pristine LNCMO (51.010 Ω) due to conductive carbon enhancing the surface electronic conductivity and introduction of Mn^{3+} improving bulk electronic conductivity. The value of R_{ct} drastically decreases from 31.030 to 12.480 Ω after 1.2 wt% carbon coating (consistent with the Li^+ diffusion coefficient calculated previously) [40]. The Warburg impedance coefficient (σ_W) decreases from 18.335 to 11.177 Ω cm^2

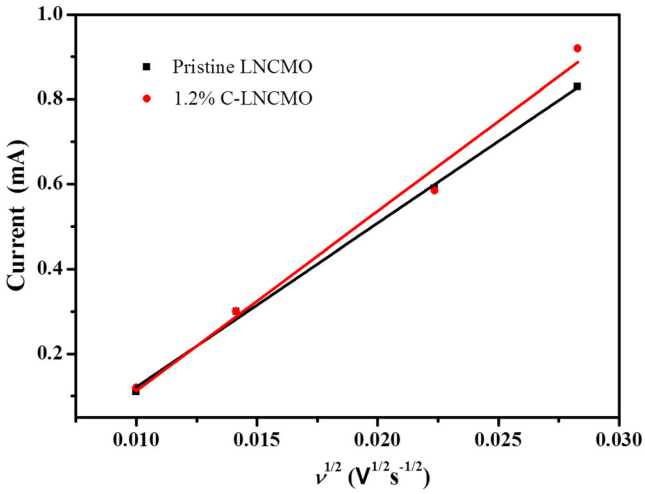

Fig. 9 Relationship between the peak current and the square root of sweep rate of the pristine LNCMO and 1.2 % C-LNCMO electrodes

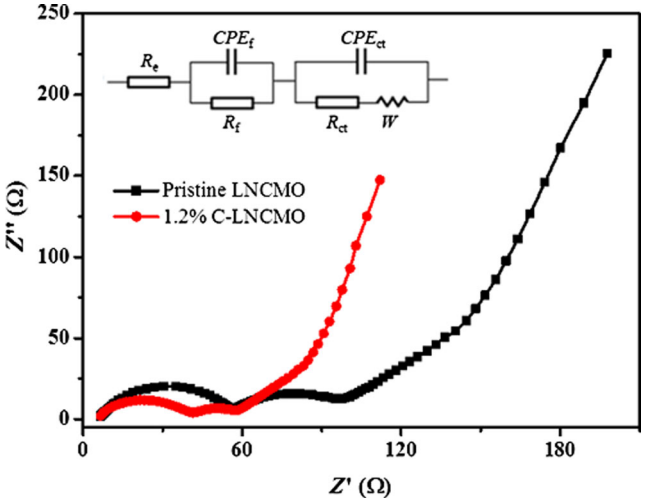

Fig. 10 Nyquist impedance spectra of the pristine LNCMO and 1.2 % C-LNCMO electrodes, the inset shows equivalent circuit for Nyquist plots

Table 2 Fitted impedance parameters of the pristine LNCMO and 1.2 % C-LNCMO

Sample	R_e (Ω)	R_f (Ω)	R_{ct} (Ω)	σ_W (Ω cm^2 s$^{-1/2}$)
Pristine LNCMO	6.377	51.010	31.030	18.335
1.2 % C-LNCMO	5.684	34.650	12.480	11.177

$s^{-1/2}$ after 1.2 % carbon coating due to the improved ionic conductivity.

Conclusions

Coating the Li-rich layered oxide cathode material with small amounts of conductive carbon has realized by the sucrose carbonization. Appropriate coated carbon layer cannot only increase the electronic conductivity at the interface with electrolyte but also improve bulk electronic conductivity and ionic conductivity by reducing small amounts of Mn^{4+} to Mn^{3+}. As a result, not only the initial coulombic efficiency and rate capability of the LNCMO have been significantly improved but also the discharge voltage fading has been mitigated by carbon coating. The carbon coating is experimentally proved as a very effective way for improving the electrochemical performance of $Li_{1.2}Ni_{0.13}Co_{0.13}Mn_{0.54}O_2$, and the appropriate carbon-coated $Li_{1.2}Ni_{0.13}Co_{0.13}Mn_{0.54}O_2$ is a promising cathode candidate for advanced lithium ion batteries.

Acknowledgments This study was supported by National Science Foundation of China (grant nos. 21006033 and 51372060) and the Fundamental Research Funds for the Central Universities (2013HGCH0002).

References

1. Yang J, Cheng F, Zhang X, Gao H, Tao Z, Chen J (2014) Porous $0.2Li_2MnO_3 \cdot 0.8LiNi_{0.5}Mn_{0.5}O_2$ nanorods as cathode materials for lithium-ion batteries. J Mater Chem A 2:1636–1640
2. Yabuuchi N, Yoshii K, Myung S-T, Nakai I, Komaba S (2011) Detailed studies of a high-capacity electrode material for rechargeable batteries, Li_2MnO_3–$LiCo_{1/3}Ni_{1/3}Mn_{1/3}O_2$. J Am Chem Soc 133: 4404–4419
3. Cheng F, Xin Y, Chen J, Lu L, Zhang X, Zhou H (2013) Monodisperse $Li_{1.2}Mn_{0.6}Ni_{0.2}O_2$ microspheres with enhanced lithium storage capability. J Mater Chem A 1:5301–5308
4. Jung YS, Lu P, Cavanagh AS, Ban C, Kim G-H, Lee S-H, George SM, Harris SJ, Dillon AC (2013) Unexpected improved performance of ALD coated $LiCoO_2$/Graphite Li-ion batteries. Adv Energy Mater 3:213–219
5. Prada E, Domenico DD, Creff Y, Bernard J, Moynot VS, Huet F (2012) Simplified electrochemical and thermal model of $LiFePO_4$-graphite Li-ion batteries for fast charge applications. J Electrochem Soc 159:A1508–A1519
6. Penki TR, Shanmughasundaram D, Jeyaseelan AV, Subramani AK, Munichandraiah N (2014) Polymer template assisted synthesis of porous $Li_{1.2}Mn_{0.53}Ni_{0.13}Co_{0.13}O_2$ as a high capacity and high rate capability positive electrode material. J Electrochem Soc 161:A33–A39
7. Jiang Y, Yang Z, Luo W, Hu X-L, Zhang W-X, Huang Y-H (2012) Facile synthesis of mesoporous $0.4Li_2MnO_3 \cdot 0.6LiNi_{2/3}Mn_{1/3}O_2$ foams with superior performance for lithium-ion batteries. J Mater Chem 22:14964–14969
8. Thackeray MM, Kang S-H, Johnson CS, Vaughey JT, Benedek R, Hackney SA (2007) Li_2MnO_3-stabilized $LiMO_2$ (M=Mn, Ni, Co) electrodes for high energy lithium-ion batteries. J Mater Chem 17: 3112–3125
9. Johnson CS, Li N, Lefief C, Thackeray MM (2007) Anomalous capacity and cycling stability of $xLi_2MnO_3 \cdot (1-x)LiMO_2$ electrodes (M=Mn, Ni, Co) in lithium batteries at 50 °C. Electrochem Commun 9:787–795
10. Liu J, Manthiram A (2010) Functional surface modifications of a high capacity layered $Li[Li_{0.2}Mn_{0.54}Ni_{0.13}Co_{0.13}]O_2$ cathode. J Mater Chem 20:3961–3967
11. Hy S, Felix F, Rick J, Su W-N, Hwang BJ (2014) Direct in situ observation of Li_2O evolution on Li-rich high-capacity cathode material, $Li[Ni_{(x)}Li_{((1-2x)/3)}Mn_{((2-x)/3)}]O_2$ ($0 \le x \le 0.5$). J Am Chem Soc 136:999–1007
12. Meng H, Jin H, Gao J, Zhang L, Xu Q (2014) Pr_6O_{11}-coated high capacity layered $Li[Li_{0.17}Ni_{0.17}Co_{0.10}Mn_{0.56}]O_2$ as a cathode material for lithium ion batteries. J Electrochem Soc 161:A1564–A1571
13. Zhang HZ, Qiao QQ, Li GR, Ye SH, Gao XP (2012) Surface nitridation of Li-rich layered $Li(Li_{0.17}Ni_{0.25}Mn_{0.58})O_2$ oxide as cathode material for lithium-ion battery. J Mater Chem 22:13104–13109
14. Martha SK, Nanda J, Veith GM, Dudney NJ (2012) Electrochemical and rate performance study of high-voltage lithium-rich composition: $Li_{1.2}Mn_{0.525}Ni_{0.175}Co_{0.1}O_2$. J Power Sources 199:220–226
15. Li ZD, Zhang YC, Xiang HF, Ma XH, Yuan QF, Wang QS, Chen CH (2013) Trimethyl phosphite as an electrolyte additive for high-voltage lithium-ion batteries using lithium-rich layered oxide cathode. J Power Sources 240:471–475
16. Wu Y, Manthiram A (2006) High capacity, surface-modified layered $Li[Li_{(1-x)/3}Mn_{(2-x)/3}Ni_{x/3}Co_{x/3}]O_2$ cathodes with low irreversible capacity loss. Electrochem Solid State Lett 9:A221–A224
17. Yuan W, Zhang HZ, Liu Q, Li GR, Gao XP (2014) Surface modification of $Li(Li_{0.17}Ni_{0.2}Co_{0.05}Mn_{0.58})O_2$ with CeO_2 as cathode material for Li-ion batteries. Electrochim Acta 135:199–207
18. Amalraj F, Talianker M, Markovsky B, Burlaka L, Leifer N, Goobes G, Erickson EM, Haik O, Grinblat J, Zinigrad E, Aurbach D, Lampert JK, Shin J-Y, Dobrick MS, Garsuch A (2013) Studies of Li and Mn-rich $Li_x[MnNiCo]O_2$ electrodes: electrochemical performance, structure, and the effect of the aluminum fluoride coating. J Electrochem Soc 160:A2220–A2233
19. Liu J, Wang Q, Jayan BR, Manthiram A (2010) Carbon-coated high capacity layered $Li[Li_{0.2}Mn_{0.54}Ni_{0.13}Co_{0.13}]O_2$ cathodes. Electrochem Commun 12:750–753
20. Shi SJ, Tu JP, Mai YJ, Zhang YQ, Gu CD, Wang XL (2012) Effect of carbon coating on electrochemical performance of $Li_{1.048}Mn_{0.381}Ni_{0.286}Co_{0.286}O_2$ cathode material for lithium-ion batteries. Electrochim Acta 63:112–117
21. Deng YH, Liu SQ, Liang XX (2013) Study of carbon surface-modified $Li[Li_{0.2}Mn_{0.54}Ni_{0.13}Co_{0.13}]O_2$ for high-capacity lithium ion battery cathode. J Solid State Electrochem 17:1067–1075
22. Nayak PK, Grinblat J, Levi M, Aurbach D (2014) Electrochemical and structural characterization of carbon coated $Li_{1.2}Mn_{0.56}Ni_{0.16}Co_{0.08}O_2$ and $Li_{1.2}Mn_{0.6}Ni_{0.2}O_2$ as cathode materials for Li-ion batteries. Electrochim Acta 137:546–556
23. Oh SW, Myung S-T, Oh S-M, Oh KH, Amine K, Scrosati B, Sun Y-K (2010) Double carbon coating of $LiFePO_4$ as high rate electrode for rechargeable lithium batteries. Adv Mater 22:4842–4845

24. Lee S, Cho Y, Song H-K, Lee KT, Cho J (2012) Carbon-coated single-crystal $LiMn_2O_4$ nanoparticle clusters as cathode material for high-energy and high-power lithium-ion batteries. Angew Chem Int Ed 51:8748–8752
25. Patey TJ, Büchel R, Ng SH, Krumeich F, Pratsinis SE, Novák P (2009) Flame co-synthesis of $LiMn_2O_4$ and carbon nanocomposites for high power batteries. J Power Sources 189:149–154
26. Yang T, Zhang N, Lang Y, Sun K (2011) Enhanced rate performance of carbon-coated $LiNi_{0.5}Mn_{1.5}O_4$ cathode material for lithium ion batteries. Electrochim Acta 56:4058–4064
27. Sinha NN, Munichandraiah N (2009) Synthesis and characterization of carbon-coated $LiNi_{1/3}Co_{1/3}Mn_{1/3}O_2$ in a single step by an inverse microemulsion route. ACS Appl Mater Inter 1:1241–1249
28. Zheng JM, Li J, Zhang ZR, Guo XJ, Yang Y (2008) The effects of TiO_2 coating on the electrochemical performance of $Li[Li_{0.2}Mn_{0.54}Ni_{0.13}Co_{0.13}]O_2$ cathode material for lithium-ion battery. Solid State Ionics 179:1794–1799
29. Wu Y, Murugan AV, Manthiram A (2008) Surface modification of high capacity layered $Li[Li_{0.2}Mn_{0.54}Ni_{0.13}Co_{0.13}]O_2$ cathodes by $AlPO_4$. J Electrochem Soc 155:A635–A641
30. Song B, Lai MO, Liu Z, Liu H, Li L (2013) Graphene-based surface modification on layered Li-rich cathode for high-performance Li-ion batteries. J Mater Chem A 1:9954–9965
31. Kunduraci M, Sharab JA, Amatucci G (2006) High-power nanostructured $LiMn_{2-x}Ni_xO_4$ high-voltage lithium-ion battery electrode materials: electrochemical impact of electronic conductivity and morphology. Chem Mater 18:3585–3592
32. Bettge M, Li Y, Gallagher K, Zhu Y, Wu Q, Lu W, Bloom I, Abraham DP (2013) Voltage fade of layered oxides: its measurement and impact on energy density. J Electrochem Soc 160:A2046–A2055
33. Zheng JM, Gu M, Genc A, Xiao J, Xu P, Chen XL, Zhu ZH, Zhao WB, Pullan L, Wang CM, Zhang J-G (2014) Mitigating voltage fade in cathode materials by improving the atomic level uniformity of elemental distribution. Nano Lett 14:2628–2635
34. Bloom I, Trahey L, Abouimrane A, Belharouak I, Zhang X, Wu Q, Lu W, Abrahama DP, Bettge M, Elam JW, Meng X, Burrell AK, Ban C, Tenent R, Nanda J, Dudney N (2014) Effect of interface modifications on voltage fade in $0.5Li_2MnO_3 \cdot 0.5\ LiNi_{0.375}Mn_{0.375}Co_{0.25}O_2$ cathode materials. J Power Sources 249:509–514
35. Song B, Liu H, Liu Z, Xiao P, Lai MO, Lu L (2013) High rate capability caused by surface cubic spinels in Li-rich layer-structured cathodes for Li-ion batteries. Sci Rep 3:3094–3105
36. Croy JR, Kim D, Balasubramanian M, Gallagher K, Kang S-H, Thackeray MM (2012) Countering the voltage decay in high capacity $xLi_2MnO_3 \cdot (1-x)LiMO_2$ electrodes (M=Mn, Ni, Co) for Li^+-ion batteries. J Electrochem Soc 159:A781–A790
37. Rui XH, Ding N, Liu J, Li C, Chen CH (2010) Analysis of the chemical diffusion coefficient of lithium ions in $Li_3V_2(PO_4)_3$ cathode material. Electrochim Acta 55:2384–2390
38. Wu X, Li H, Fei H, Zheng C, Wei M (2014) Facile synthesis of Li_2MnO_3 nanowires for lithium-ion battery cathodes. New J Chem 38:584–587
39. Yang X, Wang X, Wei Q, Shu H, Liu L, Yang S, Hu B, Song Y, Zou G, Hu L, Yi L (2012) Synthesis and characterization of a Li-rich layered cathode material $Li_{1.15}[(Mn_{1/3}Ni_{1/3}Co_{1/3})_{0.5}(Ni_{1/4}Mn_{3/4})_{0.5}]_{0.85}O_2$ with spherical core-shell structure. J Mater Chem 22:19666–19672
40. Bettge M, Li Y, Sankaran B, Rago ND, Spila T, Haasch RT, Petrov I, Abrahama DP (2013) Improving high-capacity $Li_{1.2}Ni_{0.15}Mn_{0.55}Co_{0.1}O_2$-based lithium-ion cells by modifying the positive electrode with alumina. J Power Sources 233:346–357